UW-Madison.
SSEC Publication No.82.06.W1.

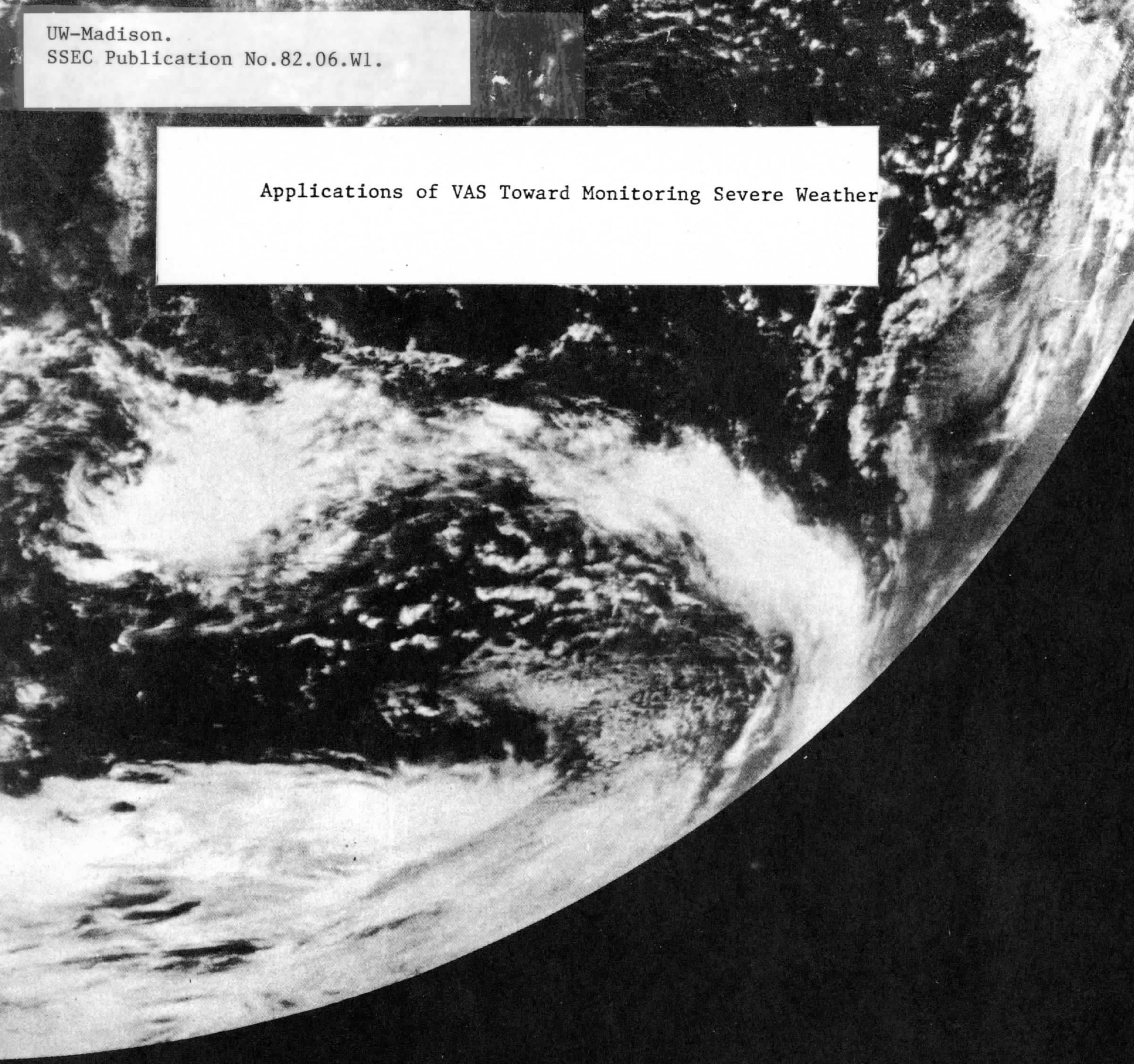

Applications of VAS Toward Monitoring Severe Weather

A REPORT

from the space science and engineering center
the university of wisconsin-madison
madison, wisconsin

Applications of VAS Toward Monitoring Severe Weather

A Report Under NASA Contract NAS5-21965

by

G. Wade, P. Menzel, and W. Smith

June 1982

The University of Wisconsin
Space Science and Engineering Center
1225 West Dayton Street
Madison, Wisconsin 53706

Since the launch of the first VISSR Atmospheric Sounder (VAS) in the fall of 1980, the Space Science and Engineering Center (SSEC) at the University of Wisconsin has been working with the National Earth Satellite Service (NESS) Development Laboratory to explore the different uses of the VAS data. This research is part of the NASA funded VAS Demonstration. High quality imagery is being achieved in twelve infrared spectral bands and in the visible; the accuracy and resolution of the derived soundings is meeting prelaunch expectations. Early assessment of the meteorological utility of the data has verified that the time sequential three-dimensional probing of the atmospheric state represents a great advance in mesometeorological observations and forecasting. This document describes some of the VAS products being generated and evaluated on the Man-computer Interactive Data Access System (McIDAS) at Wisconsin.

The twelve photographs, (found on the last three pages), taken at a McIDAS video terminal at SSEC, illustrate some of the possible uses of data from the VAS instrument. The data shown covers the period from June 1981 through March 1982 and was gathered from the VAS instrument on board GOES-5. The first set of four pictures shows imagery; the second set emphasizes some of the quantitative uses of the data gathered during the Multispectral Imaging (MSI) mode of operation, and the final set illustrates some applications of the temperature and water vapor information achieved during the Dwell Sounding (DS) mode of operation.

A full-disk image of the visible data enhanced by the longwave (11 μm) infrared window data is shown in Figure 1. The detail of the higher resolution visible is still evident, but the thermal characteristics measured by the IR are now indicated by the color tint. The coldest clouds show purple, while the warmest areas are dark red. A mid-latitude storm system is seen crossing the North Atlantic. Deep convection is present over the central and northern US. Low stratus cloud covers the Pacific near Baja, California. Some high cirrus clouds are streaking across the Pacific Northwest. Convection along the equator shows the intertropical convergence zone, and the terminator pinpoints sunrise across the central Pacific. This data, and the indicated interpretation, is standard for the operational VISSR; the VISSR data is a subset of the VAS data so by using VAS one does not sacrifice this useful and accepted tool.

Figure 2 is a full-disk image of the upper tropospheric water vapor, from the same time as Figure 1. The dark regions correspond to warmer areas, where the radiation reaching the satellite comes from lower in the atmosphere due to dryer less attenuating air above. Very deep convection is apparent here, as the central and northeastern US thunderstorms and the equatorial convection show. General subsidence (sinking, and thus drying, of the air) is seen over Baja, California. The storm crossing the North Atlantic may be steered by a jet stream core, well south of Newfoundland, which shows its left rear quadrant as the thin, dry slot over Nova Scotia. A large anticyclone (storm) in the far South Pacific dramatically shows its circulation. In imagery such as this, qualitative insights into the dynamics of the atmosphere, on synoptic and global scales, are achieved.

Figure 3 contains a side-by-side comparison of images in two wavelengths, the shortwave (3.9 μm) IR window on top and visible (0.7 μm) on bottom. Thunderstorms over the southern Mississippi Valley show up readily in the IR image, as do the thin, cirrus streamers over eastern Texas and central Mexico (they are practically undetectable in the visible image). The cold waters of the Gulf of California, the hot ground of the high plateaus in Mexico and western Texas, and the cold tops of the southern Rocky Mountains are all evident in the IR image.

Figure 4 contains a side-by-side comparison of images in two different wavelengths, 6.7 μm water vapor on top and 14 μm carbon dioxide on bottom. Both spectral bands are most sensitive to radiation from about 400 mb; thus upper level features as the Gulf thunderstorm tops and cirrus streamers are easily seen. The relatively low contrast in the 14 μm image is evidence of the small atmospheric temperature variation in this region, while the water vapor image clearly shows dry intrusions, indicating some of the dynamics of the weather.

An image of the upper tropospheric water vapor spectral band is shown in Figure 5 with contours of layer relative humidity superimposed. The relative humidity for a layer from about 300 to 500 mb, which is calculated from the radiative measurements at 6.7 μm, shows a long tongue of dry air (values less than 20%) with a minimum value over extreme western Texas (single digit values). Computations, for the coverage shown, can be completed on McIDAS within minutes after ingestion of the data.

The upper tropospheric water vapor band, with plots and contours of conventional radiosonde data, is presented in Figure 6. The wind plot at 300 mb shows a jet core over south central Texas with a maximum value of 65 meters/sec. Recalling Figure 5, one sees that the dry slot is positioned in the left rear quadrant of the jet core, where one would expect sinking (drying) motion. Therefore, frequent imaging of this upper tropospheric water vapor channel between synoptic times (12 GMT and 24 GMT) enables the jet core's position to be determined and followed.

A visible image with surface skin temperatures superimposed is found in Figure 7. Three IR spectral bands are involved in the calculation. The skin temperature is achieved by extrapolation to zero optical depth of the brightness temperatures of the water vapor window (12.7 μm), through that of the longwave window (11 μm) and through that of the most transparent shortwave window (3.9 μm). Because many areas are free of clouds for part of a day, the VAS can achieve very good sea-surface temperature coverage over a day as a result of its quasi-continuous viewing capability.

Figure 8 is a color enhanced image of the longwave window with contours of surface skin temperature (as plotted in previous figure) achieved from a single VAS image. The hot ground along the coast from Florida to South Carolina (greater than 28°C), the warm Gulf Stream current (values to 24°C), and the cold water to the north of Cape Hatteras are all clearly shown. Such sea-surface temperatures from VAS agree with buoy and other conventional measurements.

The longwave window channel is shown in Figure 9 with a plot of VAS retrievals (full profile sounding of the atmosphere) and conventional radiosondes. This display illustrates the higher horizontal resolution (50-100 km) of the VAS retrievals (shown by 700 mb temperature values), compared to the network of radiosonde stations (indicated by 700 mb wind flags). Soundings are retrieved from the radiance measurements as follows. Several adjacent fields of view are checked to be free of cloud contamination and are spatially averaged. Using a first guess profile (from climatology, radiosonde data, a numerical prediction model or previous VAS data), the radiance measurements associated with the guess atmospheric condition are calculated. These calculated values are then compared to the actual measurements. The guess profile is adjusted by an iterative process until a final retrieval is obtained, which has a difference between the calculated and observed values that falls within the noise level of the data. All the retrievals are edited for spatial and meteorological consistency.

Figure 10 shows a graphic display of contours of the 300 mb flow pattern inferred through the application of the gradient wind approximation to VAS retrievals achieved at three-hourly intervals. The higher temporal resolution of the VAS data contrasts with the frequency of the conventional radiosondes available twice daily. A jet core is seen along the western Iowa-Missouri border at 1200 GMT, with a maximum wind speed of 30 meters/sec; this jet maximum is seen to propagate to the southeast during the day and intensify to 40 meters/sec. Such development could not be resolved by radiosonde data nor could the radiosonde data be timely for use at 1800 GMT.

Contours of precipitable water change and 300 mb wind speed maximum from VAS retrievals are shown in Figure 11 superimposed on a visible image. A severe weather watch box is also plotted. This display shows an application of the VAS data to severe weather forecasting. The severe weather watch box, issued by the National Severe Storm Forecast Center in Kansas City, captured the east central area of Missouri where several tornadoes struck around St. Louis. However, with use of the VAS data shown, the watch area could have been halved. Northeastern Kansas was actually in a drying condition (as shown by the decrease in the precipitable water); northeastern central Missouri showed the largest moisture influx; and the upper level jet core was moving southeastward across Missouri (as shown in the previous figure), positioning its left front quadrant over northeastern Missouri and thus creating a favorable location for upward vertical motion. The timeliness of the VAS retrievals, produced in near real-time, can be extremely useful to forecasters.

Finally, a large-scale image of hurricane Harvey is presented in Figure 12. It shows the longwave window channel, enhanced by the upper tropospheric water vapor channel, with contours of upper level relative humidity. Although the window imagery shows an extensive cloud cover, where full profile VAS retrievals would not be possible, the hurricane environment can be probed. The enhancement by the water vapor image shows a pronounced dry slot (colored in red) to the northwest of the storm which indicates a possible steering current. The relative humidity for the layer 300-500 mb quantitatively delineates this area. Environmental temperature profiles and the sea-surface temperature pattern (as shown in earlier figures) is also useful in hurricane forecasting.

Since the spring of 1982 the VAS data is being received on a daily basis in real-time at SSEC, processed to create weather information, and then forwarded within the hour to severe weather forecasting branches of the National Weather Service for evaluation of its forecast utility. This effort is part of the NOAA VAS Assessment.

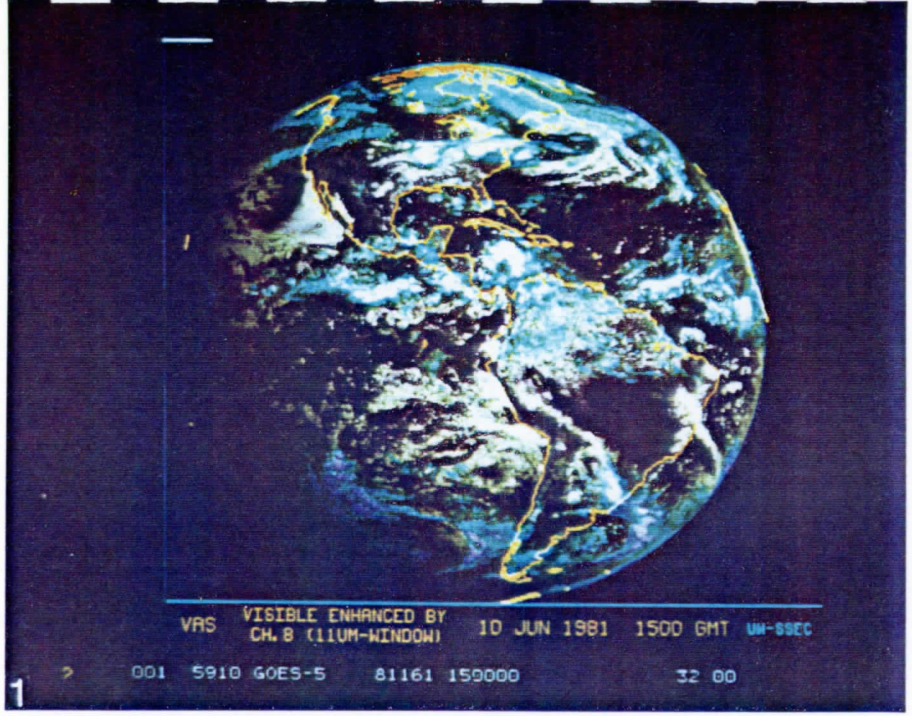
VAS VISIBLE ENHANCED BY CH.8 (11UM-WINDOW) 10 JUN 1981 1500 GMT UW-SSEC
? 001 5910 GOES-5 81161 150000 32 00

1

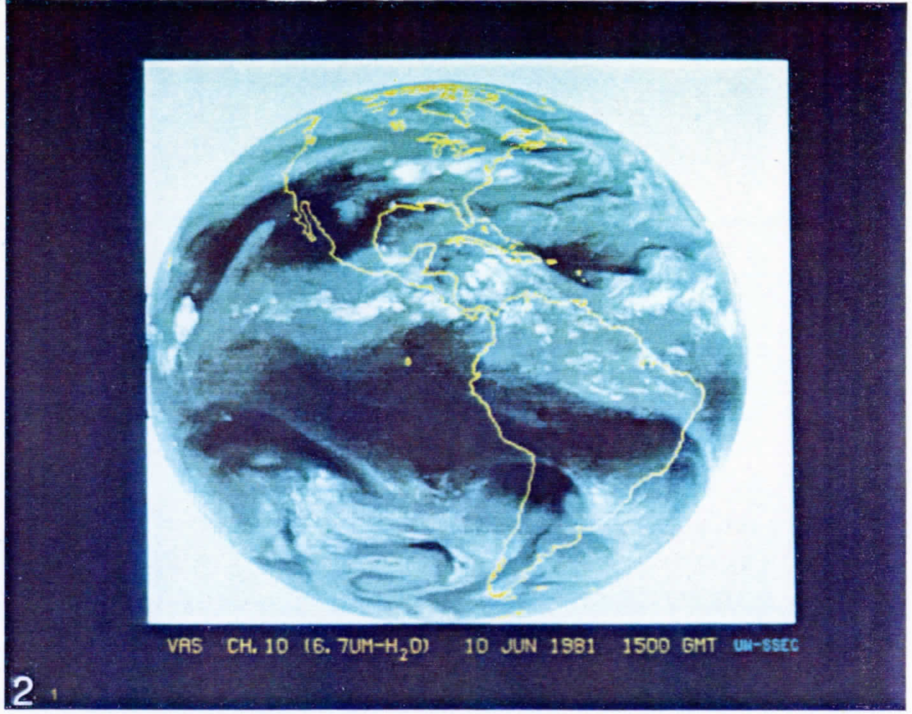
VAS CH.10 (6.7UM-H$_2$O) 10 JUN 1981 1500 GMT UW-SSEC

2

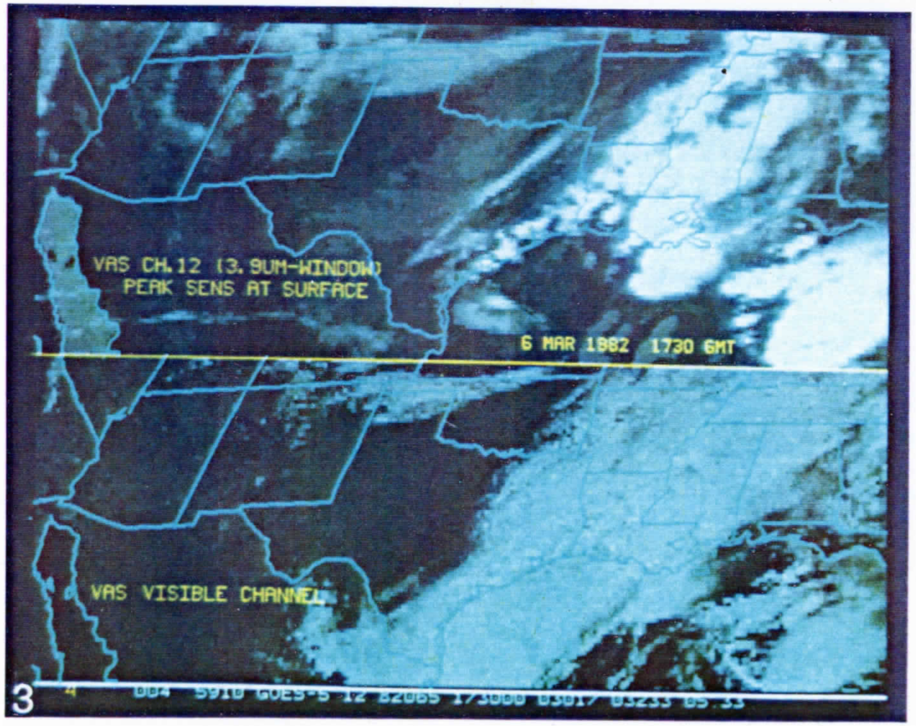
VAS CH.12 (3.9UM-WINDOW)
PEAK SENS AT SURFACE
6 MAR 1982 1730 GMT
VAS VISIBLE CHANNEL
4 004 5910 GOES-5 12 82065 173000 03017 03233 05 33

3

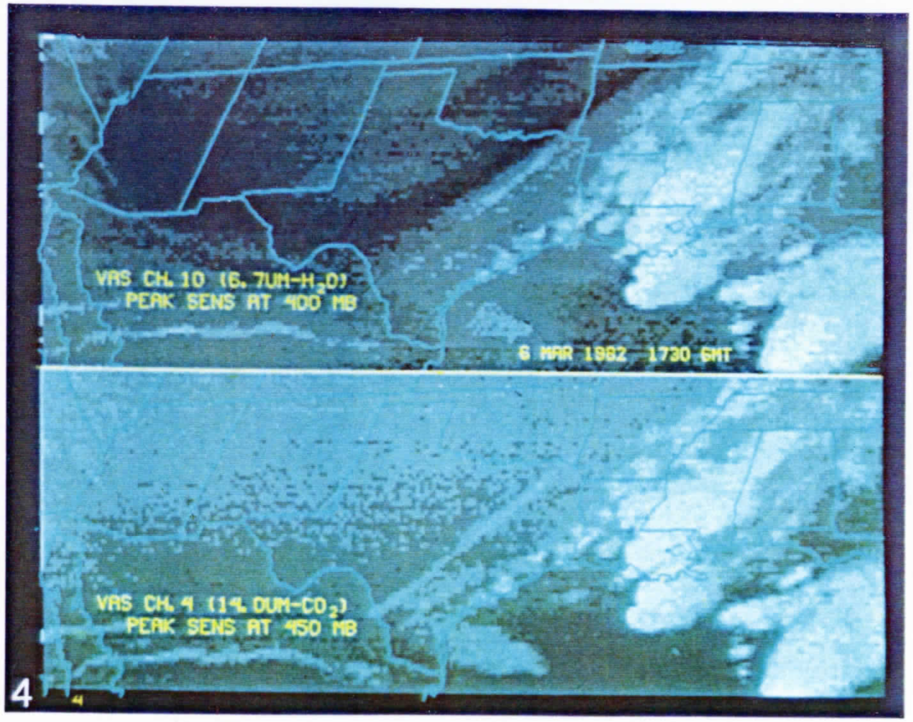
VAS CH.10 (6.7UM-H$_2$O)
PEAK SENS AT 400 MB
6 MAR 1982 1730 GMT
VAS CH.4 (14.0UM-CO$_2$)
PEAK SENS AT 450 MB

4

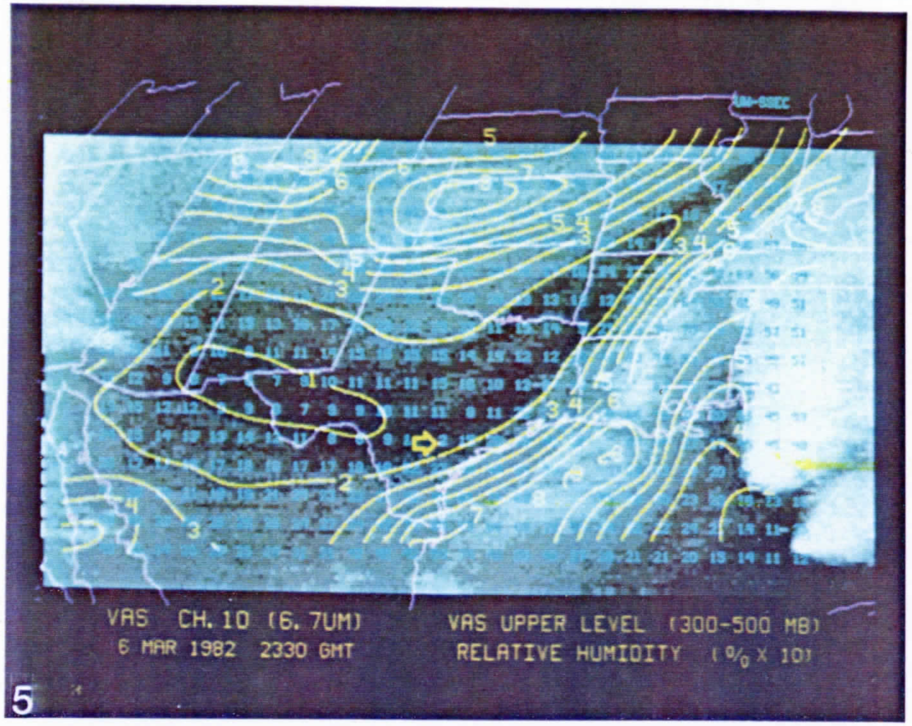
UW-SSEC
VAS CH. 10 (6.7UM)
6 MAR 1982 2330 GMT
VAS UPPER LEVEL (300-500 MB)
RELATIVE HUMIDITY (%/0 X 10)

5

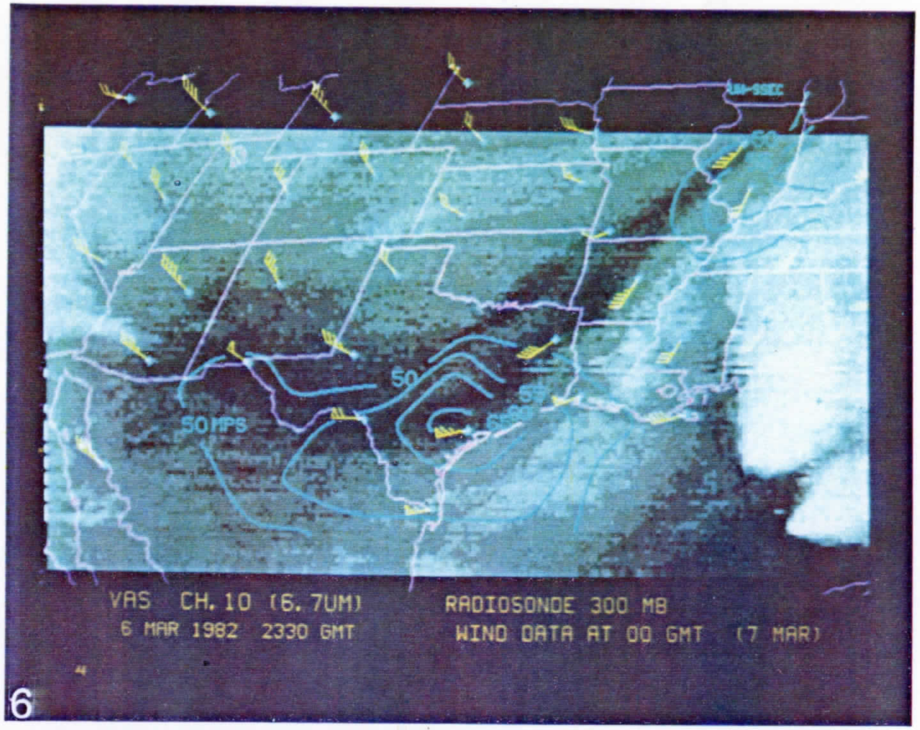
UW-SSEC
50 MPS
50
VAS CH. 10 (6.7UM)
6 MAR 1982 2330 GMT
RADIOSONDE 300 MB
WIND DATA AT 00 GMT (7 MAR)

6


(°C X 10)
SKIN
2 MAR 1982
1730 GMT
VISIBLE
SEA SFC TEMP
FROM VAS
UW-SSEC
003 5910 GOES-5 82061 173000 02808 06770 02.66

7

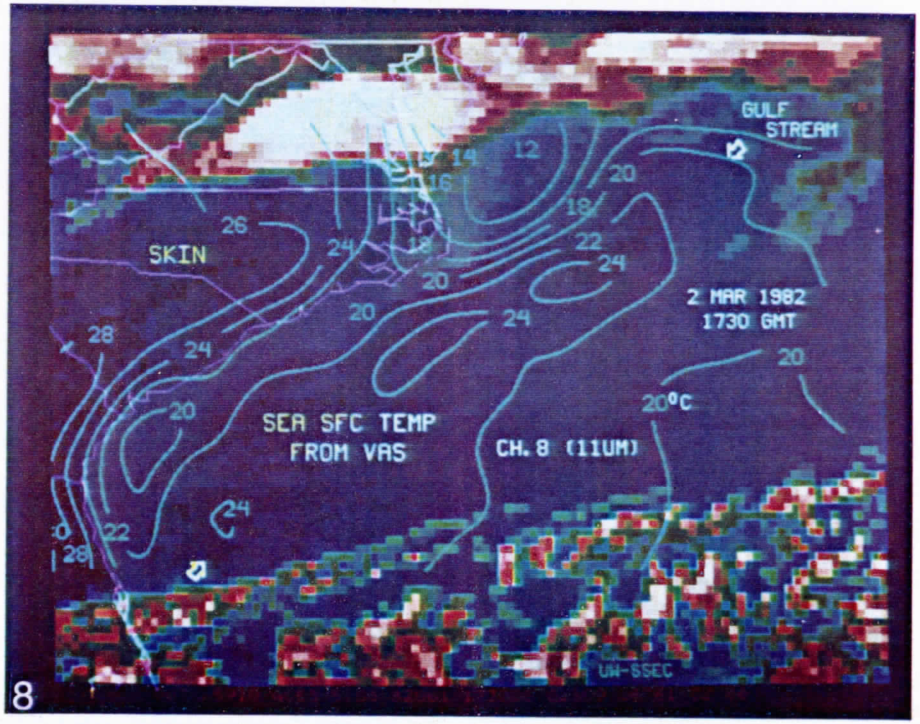
GULF
STREAM
SKIN
2 MAR 1982
1730 GMT
20°C
SEA SFC TEMP
FROM VAS
CH. 8 (11UM)
UW-SSEC

8

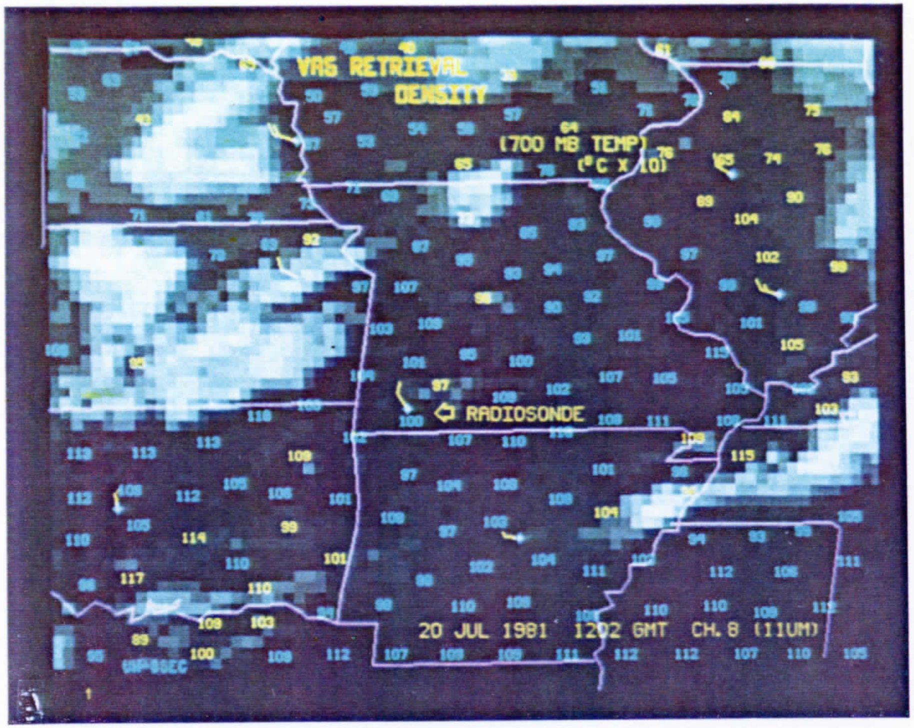
VAS RETRIEVAL DENSITY
(700 MB TEMP) (°C X 10)
RADIOSONDE
20 JUL 1981 1202 GMT CH. 8 (11UM)
UW-SSEC

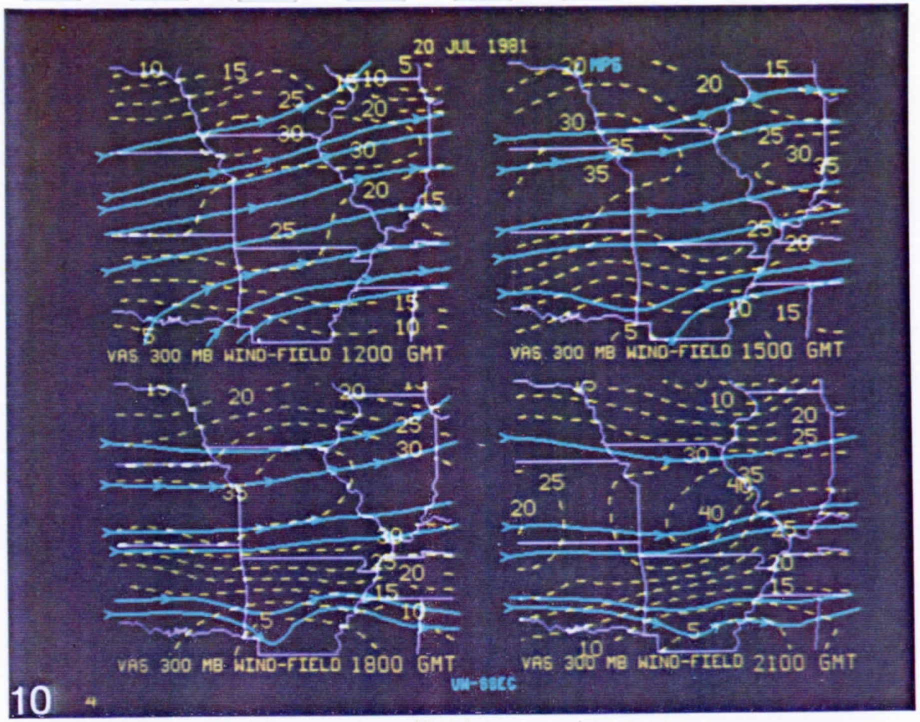

10

20 JUL 1981
20 MPS
VAS 300 MB WIND-FIELD 1200 GMT
VAS 300 MB WIND-FIELD 1500 GMT
VAS 300 MB WIND-FIELD 1800 GMT
VAS 300 MB WIND-FIELD 2100 GMT
UW-SSEC

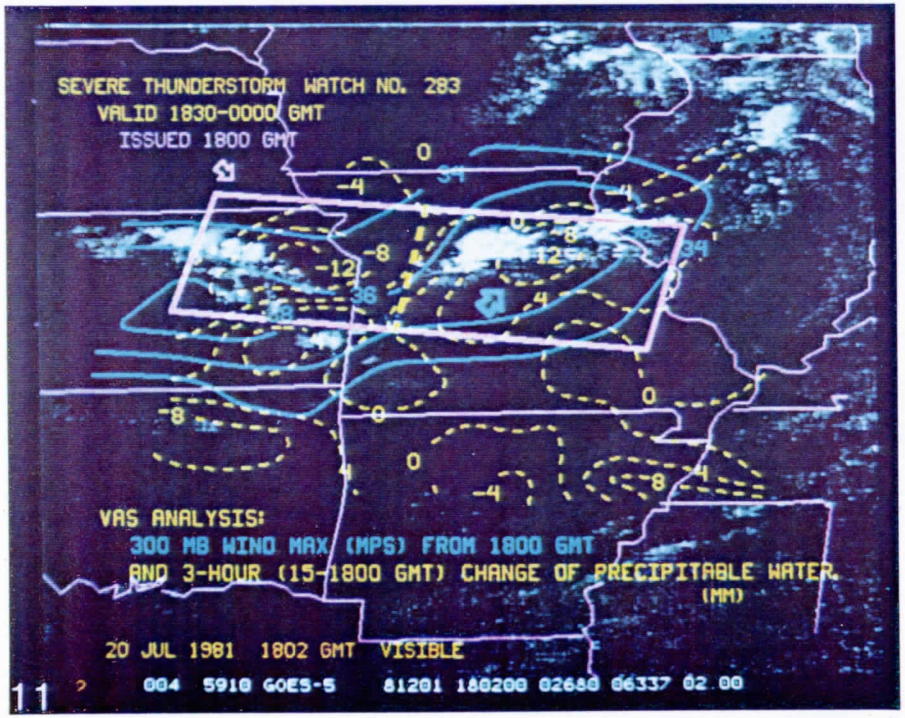

11

SEVERE THUNDERSTORM WATCH NO. 283
VALID 1830-0000 GMT
ISSUED 1800 GMT
VAS ANALYSIS:
300 MB WIND MAX (MPS) FROM 1800 GMT
AND 3-HOUR (15-1800 GMT) CHANGE OF PRECIPITABLE WATER. (MM)
20 JUL 1981 1802 GMT VISIBLE
004 5910 GOES-5 81201 180200 02680 06337 02.00

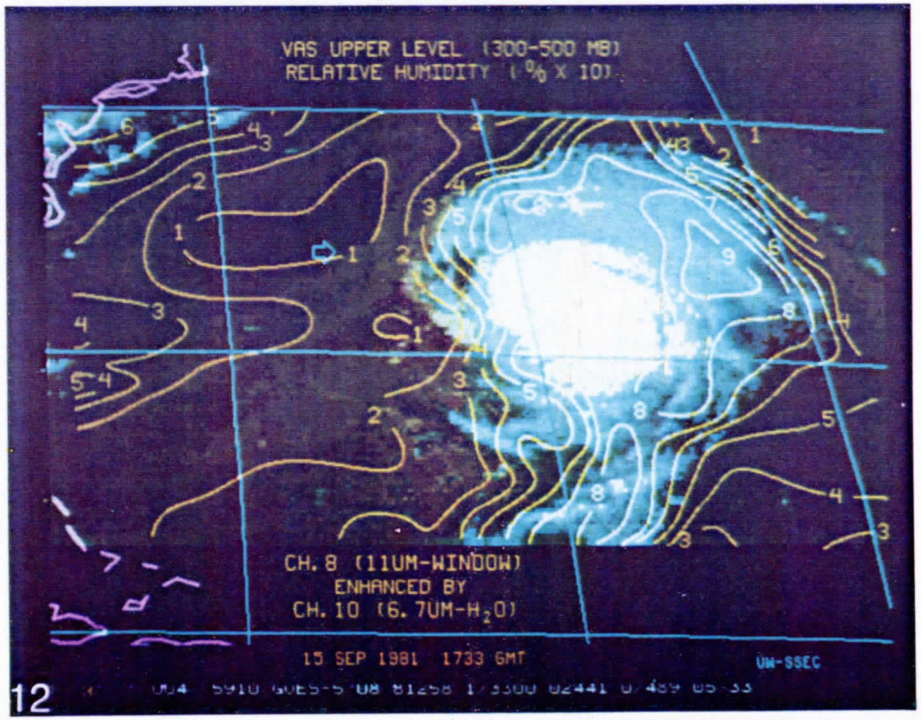

12

VAS UPPER LEVEL (300-500 MB)
RELATIVE HUMIDITY (% X 10)
CH. 8 (11UM-WINDOW)
ENHANCED BY
CH. 10 (6.7UM-H2O)
15 SEP 1981 1733 GMT
UW-SSEC